High-sensitivity refractive index sensor with normal incident geometry using a subwavelength grating operating near the ultraviolet wavelength

Yuusuke Takashima*[a, b], Masanobu Haraguchi [a], Yoshiki Naoi [a]

[a] Graduate School of Technology, Industrial and Social Science, Tokushima University, 2-1 Minami-Josanjima, Tokushima 770-8506, Japan

[b] Research Fellow of Japan Society for the Promotion of Science, Japan Society for the Promotion of Science, 5-3-1 Kojimachi, Chiyoda, Tokyo 102-0083, Japan

*Corresponding author:
E-mail: takashima@ee.tokushima-u.ac.jp
Phone: +81 88 656 7447
Fax: +81 88 656 7447

Abstract

A high-sensitivity refractive index sensor is demonstrated for the first time, near the ultraviolet (UV) wavelength region using a Si_3N_4-subwavelength grating (SWG) with a normal incident optical geometry. Using the eigenmode within the Si_3N_4-SWG, a high sensitivity for the refractive index is expected by finite-difference time-domain calculation, without an oblique incident geometry. The proposed SWG is fabricated and the high-sensitivity refractive index sensor operating near the UV wavelength is experimentally and successfully developed. The normal transmitted intensity through the fabricated SWG varies considerably with slight changes in the refractive index. The experimental sensitivity of the SWG attained 1240 % per refractive index unit (RIU) and the sensitivity shows good agreement with the calculation. These experimental results suggest that our refractive index sensor with a normal incident geometry can measure a refractive index change of 8.06×10^{-4} RIU, if the optical detection system can measure an intensity change of 1%.

Keywords: subwavelength, refractive index sensor, grating

Highlights:

- A normal incident-type refractive index sensor with an SWG was numerically designed.
- A high-sensitivity refractive index sensor with a normal incident geometry was experimentally developed near the ultraviolet wavelength region.
- The experimental sensitivity and resolution of the refractive index sensing reached 1240 % RIU^{-1}.
- A resolution of 8.06 x 10^{-4} was achieved for the refractive index sensing, using our SWG, assuming a spectrometer detection limitation of 1% for the intensity changes.

1. Introduction

High-sensitivity refractive index sensors are beneficial for various applications in several fields including bioassays, and gas and chemical sensors. These applications require high sensitivity as well as a compact device for integration. The coupling of an evanescent wave with surface-plasmon (SP) at metal or dielectric continuous film surfaces was widely employed for measuring minuscule changes of the refractive index [1-6] because the coupling condition between the evanescent wave and the SP was extremely sensitive to the refractive index of the environment around the surface. Generally, a refractive index sensor using SP requires a prism coupler, whose size is bulky for integration applications, for coupling light with the SP. Localized-surface-plasmon (LSP) in metal nanoparticles was used for the development of refractive index sensors without prism couplers [7-9]. Compact LSP refractive index sensors are suitable for integrated devices. Several groups have reported high-sensitivity refractive index sensors using guided-mode resonance [10,11], photonic crystals [12,13], diffraction from the phase grating [14], an evanescent-field-coupling guided mode [15], a Bloch surface wave [16,17], and a ring resonator [18]. However, a complex and specialized experimental setup, for example an oblique incident geometry, is still required for the optimal performance of these sensors.

Very recently, a high-contrast SWG bio-sensor with a surface-normal-coupling optical

geometry was reported at the infrared (IR) wavelength region [19]. The high-contrast SWG is composed of a high refractive index grating surrounded by a low refractive index medium. In a high-contrast SWG, the normal incident light wave can excite and interact with the multiorder eigenmodes owing to its high refractive index modulation. Utilizing this interaction, extraordinary properties such as high polarization selectivity, high-quality-factor resonance, and ultra-broadband high reflectivity with a large fabrication tolerance were obtained [20-25]. The interaction between the incident light and the eigenmode also depends on the changes in the environment around the grating because the eigenstates of the mode strongly reflect the refractive index contrast between the grating and the surrounding material. As a result, the refractive index of the surrounding material can be measured with a high sensitivity. Refractive index sensors were typically used in aqueous environments such as bioassays. For these applications, a low absorption of the light in water is desired for an improvement in the signal-to-noise (S/N) ratio. Although light near the UV wavelength range is suitable for a high S/N ratio due to its low absorption in water [26], the fabrication of an SWG sensor operating near the UV wavelength region can still be technically difficult and challenging, owing to the small grating period.

In this work, a high-sensitivity refractive index sensor with a normal incident geometry is experimentally demonstrated, using an SWG operating near the UV wavelength, for the first time. The SWG structure is designed for the high-sensitivity refractive index sensor using the wave number dispersion relationship, which determines the phase of the eigenmodes. We calculated the electromagnetic filed distribution within the designed SWG, using the finite difference time domain (FDTD) method, in order to estimate the performance of the SWG as a refractive index sensor. Further, we fabricated the designed SWG by electron beam (EB) lithography technique and the fabricated SWG sensor experimentally measured a fourth order-decimal change of the environmental refractive index, without an oblique incident geometry.

2. SWG design for the refractive index sensor

Figure 1 shows the schematic of the SWG structure. The SWG was arranged on a glass substrate with a shorter period than the incident wavelength and the grating was surrounded by material with a refractive index, n_s. The incident light was assumed to be a p-polarized plane wave in which the electric field was perpendicular to the grating stripes. The incident wavelength (λ) was set to 380 nm because of its low absorption in an aqueous environment [26].

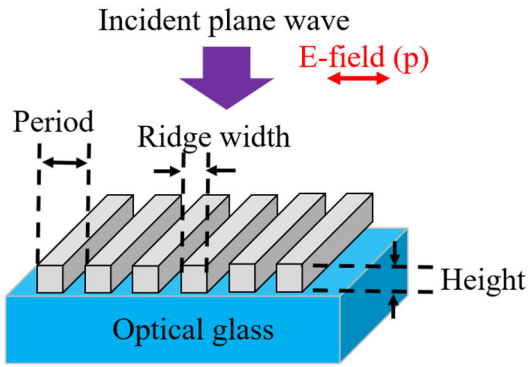

Figure 1 Schematic the SWG refractive index sensor

The operating principle of the refractive index sensor, using the SWG, is as follows: In the SWG, the eigenmode exists as a solution for Maxwell's equations in the periodic refractive index distribution. If the refractive index contrast between the grating ridges and air gaps is large, the incident light excites not only the fundamental mode but also the higher-order modes owing to a large modulation of the refractive index. These modes are coupled with each other at the interface between the SWG and the optical glass, and the transmitted light through the SWG is expressed by the interference between these modes [21,22]. If these eigenmodes are anti-phase and cancel each other's amplitudes at the interface between the SWG and the optical glass, the transmitted light intensity through the SWG becomes nil. The transmitted light intensity sensitively varies with the changes in the environmental refractive index around the SWG because

the eigenmode phases strongly depended on the refractive index contrast between the grating and the surrounding material. As a result, slight changes in the refractive index of the surrounding materials can be measured, without an oblique incident geometry.

Based on the above operating principle, we designed the SWG for the refractive index sensor using the wave number dispersion curve of the eigenmode, which determined the phase of the mode [22]. Sufficient refractive index contrast between the grating ridges and air gaps is required for the excitation of the higher-modes to measure the refractive index because the interference between the modes cannot be obtained without the higher-order modes. On the other hand, we predicted that a refractive index contrast, which is too large, is not suitable for refractive index sensing because such a contrast saturates the eigenmode phase shift and induces insensitivity to slight changes in the surrounding refractive index. Thus, we selected Si_3N_4, whose refractive index value is moderate and satisfies the above requirements, as the SWG material (the refractive index of Si_3N_4 is 2.0847 at a 380-nm wavelength) [27]. In addition, Si_3N_4 is chemically stable for various environment and is suitable for the SWG sensor material. We also considered the dependency of the dispersion curve on the n_s value, which is closely related to the sensor sensitivity. The sensitivity of this proposed sensor device is subject to propagation properties of the excited eigenmodes, because the dependency of the mode phase on variation of the environmental refractive index strongly influences on the interference between the modes. The phase shift of the mode is not constant for changes in n_s because of the corresponding nonlinear variations of the dispersion curve [22]. If the dispersion curve varies considerably with slight changes in n_s, the mode phase also shifts rapidly. Thus, a high sensitivity for the sensor can be expected, without an oblique incident system.

Based on this, grating parameters such as the grating period (Λ), grating height (H), and the grating width (w) were designed using the wave number dispersion curve of the eigenmode

in order to obtain a high sensor sensitivity. As a result, these parameters were set to Λ = 215 nm, H = 150 nm, and w = 150 nm, respectively.

To estimate the sensor performance of the designed Si_3N_4-SWG, the electromagnetic filed distribution of the SWG was calculated by the FDTD method (Fullwave: R-soft).

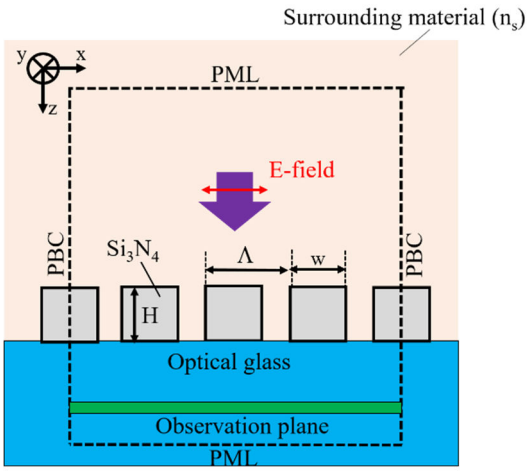

Figure 2 FDTD numerical calculation model of the SWG refractive index sensor

Figure 2 shows the FDTD numerical calculation model. In this model, the Si_3N_4 grating ridges were arranged on an optical glass and the ridges were surrounded by a medium with a refractive index, n_s. The length of the grating stripe along the y-direction was assumed to be infinite because the actual length was considerably larger than the incident wavelength. 20 number perfect matched layers (PMLs) and the periodic boundary condition (PBC) were employed for the z- and x-directions, respectively. The calculation region was defined as the boundaries depicted in Fig. 2. The vertical and lateral sizes of the calculation region were 1550 nm and 860 nm, respectively and the region was divided into 2 nm x 2 nm square cells. The incremental time step was 0.4656 x 10^{-13} s. A p-polarized incident plane wave with a wavelength of 380 nm was made to normally

enter the designed SWG. The incident light propagated along +z direction from the surrounding material to the glass substrate. The transmitted intensity at the observation plane was evaluated by a Poynting vector, when the value of n_s was varied. Figure 3 shows the transmitted light intensity through the designed Si_3N_4-SWG as a function of the n_s value. The value, n_s = 1.3406, corresponds to that of pure water [26] and the transmitted intensities in Fig. 3 were normalized at this value. In Fig. 3, the transmitted intensity rapidly decreases with minuscule changes in the refractive indices in the region, n_s = 1.3406–1.3900. The inclination of the transmitted intensity per refractive index unit (RIU) indicates the sensor sensitivity. We obtained various sensitivities for the designed Si_3N_4-SWG, as shown in Fig. 3; they were 1449% RIU^{-1}, 1232% RIU^{-1}, and 2195% RIU^{-1} for the n_s = 1.3406–1.3420, n_s = 1.3440–1.3470, and n_s = 1.3500–1.3900 refractive index ranges, respectively. These results imply that the refractive-index-sensing resolution with the SWG attains a value of 8.116 x 10^{-4} RIU at least, if the optical detection system can measure an intensity change of 1%. The variation in the sensitivity maybe owing to the nonlinear variation of the dispersion curve, for changes in n_s. These numerical results indicate that a high-sensitivity refractive index sensor near the ultraviolet wavelength can be successfully achieved, without an oblique incident optical geometry.

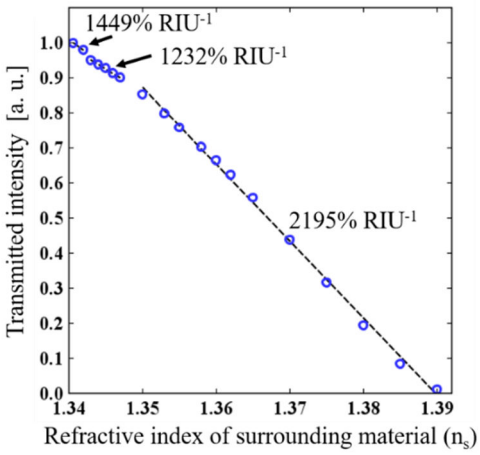

Figure 3 Transmitted intensity dependence on n_s

To reveal the origin of the high sensitivity of the designed Si_3N_4-SWG, the magnetic field distribution within the SWG at low (n_s = 1.3900) and high transmitted intensity conditions (n_s = 1.3406) are depicted in Figs. 4 (a) and (b), respectively. The magnetic field intensity is normalized by that of the light source. The green square indicates the grating ridges. For the low transmitted intensity condition in Fig. 4(a), the magnetic field distribution inside the SWG indicates that the field amplitude within the grating ridges and air gaps at the interface between the SWG and the optical glass are out of phase and cancel each other. As a result, the transmitted field intensity is nil. In contrast, the amplitudes at the grating ridges and air gaps at the high transmitted intensity condition (n_s = 1.3406) are in phase and the transmitted field intensity becomes considerably larger than that in the low transmitted intensity condition, as shown in Fig. 4(b). These calculated fields can explain the origin of the high sensitivity of the designed SWG sensor. The phases of the existing modes closely reflect the refractive index contrast between the grating ridges and the surrounding media. The interference between the modes is determined not only by the phase of the individual modes but by those of all the existing modes also. Thus, the transmitted intensity is highly sensitive for slight changes in n_s, even with a normal incident optical geometry because the phase shifts of the all the existing modes contribute to the interference, for changes in n_s.

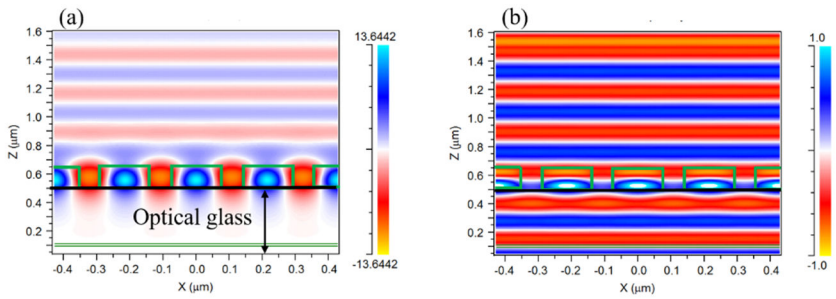

Figure 4 Magnetic field distribution at (a) low and (b) high transmittance conditions. The intensity was normalized by that of the light source. The green squares indicate the grating ridges.

3. Experimental results and discussion

We fabricated the designed Si_3N_4-SWG structure with Λ = 215 nm, H = 150 nm, and w = 150 nm on an optical glass substrate using the chemical vaper deposition (CVD), EB lithography, and inductive coupled plasma (ICP) etching techniques. A 150 nm-thick film of Si_3N_4 was deposited on the glass substrate by CVD. A 100-nm thick EB resist film was spin-coated on the Si_3N_4 film. The grating pattern was drawn by EB lithography and a patterned resist was developed. The grating area was 0.9 mm x 0.9 mm and approximately 4200 lines were present in this area. An 80 nm-thick Ni film was evaporated on the patterned resist as an etching mask and the resist was removed. ICP etching using CHF_3 gas was used to form the Si_3N_4-SWG. After the etching process, the Ni-mask was removed by nitric acid aqua. A scanning electron microscope (SEM) image of the fabricated SWG is shown in Fig. 5. The fabricated grating period and the grating stripe width were 215 nm and 150 nm, respectively. Figure 5 also shows that the sidewall of the fabricated SWG is rough and non-ideal rectangle shape, and the fluctuation of the grating stripe width is about 30 nm.

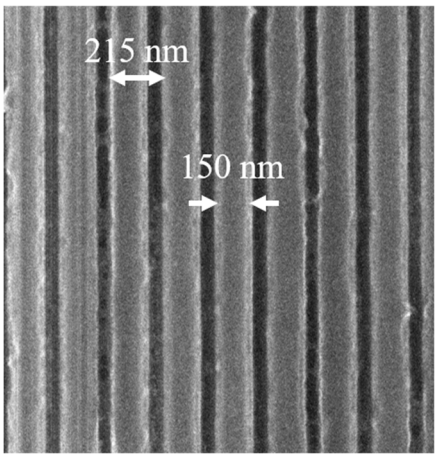

Figure 5 SEM image of the fabricated Si_3N_4-SWG

We measured the transmitted light intensity through the SWG by varying n_s, to evaluate the sensor performance. The experimental measurement set up is shown in Fig. 6. A xenon lamp was used as the near UV light source and a collimation lens was placed in front of the lamp. The incident light was p-polarized by the polarizer. The diameter of the incident light through the iris was approximately 0.8 mm. To estimate the sensitivity of the fabricated SWG for changes in n_s, ethanol solution diluted by pure water was used. The fabricated SWG was placed in a plastic cell filled with ethanol solution and p-polarized incident light with a wavelength of 380 nm was made to normally enter the grating. The mass concentration of ethanol was increased and the transmitted intensity through the SWG was measured by a spectrometer, and this measurement was done at room temperature.

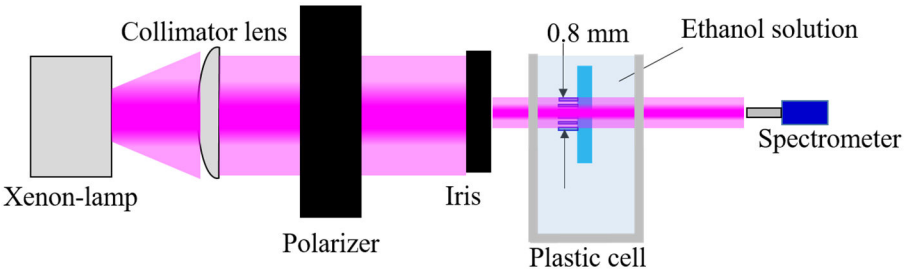

Figure 6 Experimental measurement setup

Figure 7 shows the transmitted intensity as a function of n_s. The value of n_s in Fig. 7 is derived from the mass concentration of water and ethanol; the refractive indices, n_{water} and $n_{ethanol}$, were obtained from literature (n_{water}=1.3406, $n_{ethanol}$=1.3753) [26,28]. The error bars depict the standard deviation over three measurements. In Fig. 7, a maximum transmitted light intensity is observed at n_s = 1.3406 (in pure water), which rapidly decreases with a slight increase in n_s. The transmittance at n_s=1.3406 was also about 94% of that through the glass substrate at same experimental conditions. Different sensitivities were obtained with a range of n_s values and the

experimental sensitivity of the sensor reached about 1240 % RIU^{-1} for n_s =1.3464–1.3545.The experimental results demonstrate extremely good agreement with those calculated by the FDTD method. The experimental sensitivity was slightly higher than the calculated one. The origin of the deviation maybe the non-ideal vertical shape and the rough sidewalls of the grating, resulting from the ICP etching process. These results also indicates that our SWG structure resistant to fabrication errors as mentioned in previous publication [29], and the SWG is useful for overcoming the technically difficultly in the fabrication process of a shorter wavelength operating devices. On the other hand, the flat response of the sensitivity is observed at n_s = 1.3425 to 1.3450. We consider the origin of the flat response as follows. The flat response range corresponds to the refractive index region, where the sensor sensitivity changes from 1449%RIU to 1232%RIU as shown Fig.3. This indicates the excited modes inside SWG have different phase dependences on the n_s, respectively,

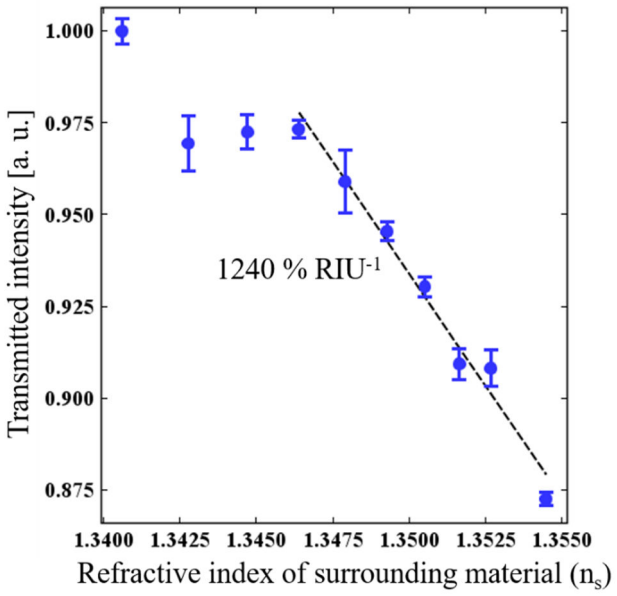

Figure 7 Experimental transmitted intensity through the fabricated Si_3N_4-SWG as a function of the refractive index of the surrounding material

because the wave number dispersion curve of the mode, which determines the mode phases, nonlinearly varied for n_s. If the relative phase relation between the modes slightly changed regardless of the phase variation of the individual modes, the interference between the modes is almost unchanged. As a result, the flat response of sensitivity is occurred.

The experimental sensitivity of the fabricated SWG corresponds to a sensor resolution of 8.06 x 10^{-4} RIU, without an oblique incident geometry, if the spectrometer can measure a 1% change in the light intensity. This is first experimental demonstration of a high-sensitivity refraction index sensor with a normal incident geometry, using an SWG operating near the ultraviolet wavelength region. The high sensing resolution and sensitivity of the fabricated Si_3N_4-SWG are comparable with those of refractive index sensors using SP resonance [2,6], guided-mode-resonance [10,11], and photonic crystals [12]. The SWG sensor demonstrated in this work does not require an oblique geometry and special measurement techniques; hence, compactness and high sensitivity can be realized simultaneously. Moreover, a high-sensitivity sensing of the refractive index can be achieved in various aquatic measurement situations because the SWG sensor is operated near the UV wavelength, with an extremely low attenuation in water. Thus, our SWG sensor is suitable for integration and practical use in many applications requiring refractive index sensing.

4. Conclusion

In conclusion, a high-sensitivity refractive index sensor with a normal incident geometry was experimentally demonstrated, using an SWG structure near the UV wavelength region. The SWG structure was designed using the wave number dispersion relationship, which determines the phase of the eigenmode. The electromagnetic field distribution within the designed SWG was

calculated by the FDTD method to estimate the sensor performance of the SWG. The calculation results demonstrated that the transmitted intensity through the SWG sensitively varied with slight changes in the refractive index of the surrounding material. The designed SWG was fabricated by the CVD, EB-lithography, and ICP-etching techniques. The transmitted light intensity through the fabricated SWG varied rapidly on increasing the refractive index of the surrounding material. The experimental sensitivity reached 1240 % RIU^{-1} indicating that this SWG sensor can measure a refractive index change of 8.06 x 10^{-4} RIU, if the optical detection system can measure an intensity change of 1%. This is first report of a high-sensitivity refractive index sensor with a normal incident geometry, using an SWG operating near the UV wavelength. This sensor is suitable for the various integration applications requiring refractive index sensing.

Acknowledgments

This work was supported by JSPS KAKENHI, Grant Number: JP16J1123210.

References

[1] J. Homola, S. S. Yee, G. Gauglitz, Surface plasmon resonance sensors: review, Sens. Actuators B 54 (1999) 3–15.

[2] C. R. Trioli, A. Trouillet, C. Veillas, H. Gagnaire, Monochromatic excitation of surface plasmon resonance in an optical–fiber refractive–index sensor, Sens. Actuators A 54 (1996) 589–593.

[3] R. Slavik, J. Homola, J. Ctyroky, Miniaturization of fiber optic surface plasmon resonance sensor, Sens. Actuators B 51 (1998) 311–315.

[4] A. A. Rifat, G. A. Mahdiraji, Y. M. Sua, R. Ahmed, Y. G. Shee, F. R. M. Adikan, Highly

sensitive multi-core flat fiber surface plasmon resonance refractive index sensor, Opt. Express 24 (2016) 2485–2495.

[5] K. Li, T. Zhamg, G. Liu, N. Zhang, M. Zhang, L. Wei, Ultrasensitive optical microfiber coupler based sensors operating near the turning point of effective group index difference, Appl. Phys. Lett. 109 (2016) 101101.

[6] D. Michel, F. Xiao, K. Alameh, A compact flexible fiber-optic surface plasmon resonance sensor with changeable sensor chips, Sens. Actuators B 246 (2017) 258–261.

[7] K. M. Mayer, J. H. Hafner, Localized surface plasmon resonance sensors, Chem. Rev. 111 (2011) 3828–3857.

[8] E. M. Larsson, J. Alegret, M. Kall, D. S. Sutherland, Sensing characteristics of NIR localized surface plasmon resonances in gold nanorings for application as ultrasensitive biosensors, Nano Lett. 7 (2007) 1256–1263.

[9] G. Li, Y. Shen, G. Xiao, C. Jin, Double-layered metal grating for high–performance refractive index sensing, Opt. Express 23 (2015) 8995–9003.

[10] J. H. Schmid, W. Sinclair, J. Garcia, S. Janz, J. Lapointe, D. Poitras, Y. Li, T. Mischki, G. Lopinski, P. Cheben, A. Dalage, A Densmore, P. Waldron, D. X. Xu, Silicon-on insulator guided mode resonant grating for evanescent field molecular sensing, Opt. Express 17 (2009) 18371–18380.

[11] A. Shakoor, M. Grande, J. Grant, D. R. S. Cumming, One-dimensional silicon nitride grating refractive index sensor suitable for integration with CMOS detectors, IEEE Photon. 9 (2017) 6800711.

[12] Y. Lin, H. M. Salemink, Photonic crystal-based all-optical on-chip sensor, Opt. Express 20 (2012) 19912–19920.

[13] A. D. Falco, L.O'Faolain, T. F. Krauss, Chemical sensing in slotted photonic crystal

heterostructure cavities, Appl. Phys. Lett. 94 (2009) 063503.

[14] P. K. Sahoo, J. Joseph, R. Yukino, A. Sandhu, High sensitivity refractive index sensor based on simple diffraction from phase grating, Opt. Lett. 41 (2016) 2101–2104.

[15] D. V. Nesterenko, S. Hayashi, Z. Sekkat, Evanescent-field-coupled guided-mode sensor based on a waveguide grating, Appl. Opt. 54 (2015) 4889–4894.

[16] X. B. Kang, L. J. Liu, H. Lu, H. D. Li, Z. G. Wang, Guided Bloch surface wave resonance for biosensor designs, J. Opt. Soc. Am. 33 (2016) 997–1003.

[17] X. B. Kang, L. W. Wen, Z. G. Wang, Design of guided Bloch surface wave resonance bio-sensors with high sensitivity, Opt. Commun. 383 (2017) 531–536.

[18] J. Flueckiger, S. Schmidt, V. Donzella, A. Sherwali, D. M. Ratner, L. Chrostowski, K. C. Cheung, Sub-wavelength grating for enhanced ring resonator biosensor, Opt. Express 24 (2016) 15672–15686.

[19] T. Sun, S. Kan, G. Marriott, C. C. Hasnain, High-contrast grating resonators for label-free detection of disease biomarkers, Sci. Rep. 6 (2016) 27482.

[20] C. F. R. Mateus, M. C. Y. Huang, Y. Deng, A. R. Neureuther, C. J. C. Hasnain, Ultrabroadband mirror using low-index cladded subwavelength grating, IEEE Photonics Technol. Lett. 16 (2004) 518–520.

[21] C. J. C. Hasnain, High-contrast grating as a new platform for integrated optoelectronics, Semicond. Sci. Technol. 26 (2011) 014043.

[22] C. J. C. Hasnain, W. Yang, High-contrast grating for integrated optoelectronics, Adv. Opt. Photonics 4 (2012) 379–440.

[23] Y. Takashima, R. Shimizu, M. Haraguchi, Y. Naoi, Polarized emission characteristics of UV-LED with subwavelength grating, Jpn. J. Appl. Phys. 53 (2014) 072101.

[24] Y. Takashima, R. Shimizu, M. Haraguchi, Y. Naoi, Influence of low-contrast subwavelength

grating shape on polarization characteristics of GaN–based light emitting-diode emissions, Opt. Eng. 54 (2015) 067112.

[25] Y. Takashima, M. Tanabe, M. Haraguchi, Y. Naoi, Highly polarized emission from a GaN-based ultraviolet light–emitting diode using Si–subwavelength grating on a SiO_2 underlayer, Opt. Commun. 369 (2016) 38–43.

[26] G. M. Hale, M. R. Querry, Optical constants of water in the 200-nm to 200-μm wavelength region, Appl. Opt. 12 (1973) 555–563.

[27] H. R. Philipp, Optical properties of silicon nitride, J. Electrochim. Soc. 120 (1973) 295–300.

[28] E. Sani, A. Dell'Oro, Spectral optical constants of ethanol and isopropanol from ultraviolet to far infrared, Optical Materials 60 (2016) 137–141.

[29] Y. Zhou, M. C. Y. Huang, C. J. C. Hasnain, Large fabrication tolerance for VCSELs using high-contrast grating, IEEE Photonics Technol. Lett. 20 (2008) 434-436.